

Anomalous Behavior of Thermodynamic Properties of Strongly Correlated Fermi Systems

J. W. Clark,¹ V. A. Khodel,^{2,1} and M. V. Zverev²

¹*McDonnell Center for the Space Sciences and Department of Physics,
Washington University, St. Louis, MO 63130, USA*

²*Russian Research Center Kurchatov Institute, Moscow, 123182, Russia*
(Dated: November 6, 2018)

Thermodynamic characteristics of Fermi systems are investigated in the vicinity of a phase transition where the effective mass diverges and the single-particle spectrum becomes flat. It is demonstrated that at extremely low temperatures T , the flattening of the spectrum is reflected in non-Fermi-liquid behavior of the inverse susceptibility $\chi^{-1}(T) \sim T^\alpha$ and the specific heat $C(T)/T \sim T^{-\alpha}$, with the critical index $\alpha = 2/3$. In the presence of an external static magnetic field H , both these quantities are found to exhibit a scaling behavior, e.g. $\chi^{-1}(T, H) = \chi^{-1}(T, 0) + T^{2/3}F(H/T)$, in agreement with available experimental data.

PACS numbers: 71.10.Hf, 71.27.+a

Manifestations of non-Fermi-liquid (NFL) behavior observed at extremely low temperatures T in a number of strongly correlated Fermi systems,^{1,2,3,4,5,6,7,8,9,10} notably ³He films and heavy-fermion metals, provide valuable clues to a fundamental microscopic understanding of these systems. This anomalous behavior is commonly attributed to antiferromagnetic spin fluctuations, and numerous strategies have been advanced (e.g. Ref. 11) based on integrating out all degrees of freedom except spin fluctuations. However, the spin-fluctuation model (SFM) is unable to reproduce the results of precise measurements of the inverse spin susceptibility, which, on the “metallic” side of the critical point, is found to obey $\chi^{-1}(T) \sim T^\alpha$ with a critical index $\alpha < 1$ (cf. Refs. 1,9,12). Difficulties are likewise encountered for the thermal expansion data.¹⁴ The SFM also fails to explain^{6,9,10,13} the scaling exhibited by $\chi(T, H)$ in external, sometimes tiny, static magnetic fields H . Moreover, the SFM falls short when confronted with other generic features revealed by experiment, most notably a divergence of the effective mass $M^*(\rho)$ at a critical density $\rho = \rho_\infty$ and the emergence of NFL features even before the critical point.^{1,3,4,5}

We are therefore compelled to explore a different strategy, in which NFL anomalies are attributed to fermionic degrees of freedom and specifically associated with flattening of the single-particle spectrum $\xi(p)$ in the immediate vicinity of ρ_∞ . Near this point, the FL formula $\xi_{FL}(p) = p_F(p - p_F)/M^*(\rho)$ must be supplemented by terms nonlinear in $p - p_F$, since $\xi_{FL}(p; \rho)$ vanishes identically at ρ_∞ . Here we shall study consequences of the alteration of $\xi(p)$ on the “metallic” side of the phase transition. Importantly, as argued below, the ratio of the damping $\gamma(\varepsilon)$ of single-particle excitations to relevant energies ε remains relatively small in this regime. Accordingly, the Landau quasiparticle formalism still applies.

We focus our attention on the real part of the AC spin susceptibility $\chi(T, \omega \rightarrow 0)$ given by the familiar FL formula¹⁵

$$\chi(T, \rho) = \chi_0(T, \rho)/[1 - g_0(\rho)\Pi_0(T, \rho)], \quad (1)$$

where g_0 is the zeroth harmonic of the Landau spin-spin interaction $\chi_0 = -\mu_B^2\Pi_0$, and μ_B is the Bohr magneton. To be definite, we treat the homogeneous three-dimensional (3D) case, with

$$\Pi_0(T) = \int \frac{dn(\xi(p))}{d\xi(p)} dv \equiv -\frac{p_F^2}{\pi^2 T} \int n(\xi)[1 - n(\xi)] \frac{dp}{d\xi} d\xi, \quad (2)$$

where $n(\xi(p)) = 1/[1 + \exp(\xi(p)/T)]^{-1}$ is the quasiparticle momentum distribution and $dv = 2d^3p/(2\pi)^3$. While Eqs. (1) and (2) are formally identical to familiar textbook formulas, the function $\Pi_0(T)$ can differ profoundly from its FL realization due to complicated character of the group velocity $d\xi(p)/dp$ in the momentum region where $|\xi(p)| \simeq T$, which is dominant in the integral (2).

To proceed, we invoke the well-known expression¹⁵

$$\frac{\partial \xi(p)}{\partial \mathbf{p}} = \frac{\mathbf{p}}{M} + \int f(\mathbf{p}, \mathbf{p}_1) \frac{\partial n(\xi(p_1))}{\partial \mathbf{p}_1} dv_1, \quad (3)$$

connecting the spectrum $\xi(p)$ and the momentum distribution $n(\xi)$ through the Landau interaction function $f(\mathbf{p}, \mathbf{p}_1)$. At $T = 0$, Eq. (3) implies that the effective mass M^* is related to the first harmonic $f_1(p_F, p_F)$ of the interaction function by

$$M/M^*(\rho, T = 0) = 1 - F_1^0(\rho)/3 \equiv D(\rho), \quad (4)$$

in which $F_1^0(\rho) = f_1(p_F, p_F)N_0$ with $N_0 = p_F M/\pi^2$. Thus $M^*(\rho, T = 0)$ diverges at the critical density ρ_∞ , where $D(\rho_\infty) = 0$, while at nonzero temperatures, $M^*(\rho_\infty, T)$ already has a finite value.¹⁶ Its T dependence is found by expanding relevant quantities on both sides of Eq. (3) in Taylor series, thereby obtaining

$$d\xi/dp \simeq p_F/M^*(\rho, T) + v_2(p - p_F)^2/Mp_F \quad (5)$$

with

$$\frac{M}{M^*(T, \rho)} = D(\rho) + \frac{M}{3p_F} \int \left[(f_1^1 p_F^2 + 2f_1 p_F)(p - p_F) \right]$$

$$+ \left(\frac{1}{2} f_1'' p_F^2 + 2 f_1' p_F + f_1 \right) (p - p_F)^2 \left] \frac{\partial n(\xi(p))}{\partial p} \frac{dp}{\pi^2}. \quad (6)$$

Here $v_2 = -p_F^3 M f_1'' / 6\pi^2$, $f_1' = [df_1(p, p_F)/dp]_{p=p_F}$, and $f_1'' = [d^2 f_1(p, p_F)/dp^2]_{p=p_F}$. The term $v_1(\rho)(p - p_F)$, which provides the contribution $v_1(\rho)(p - p_F)^2/2$ to $\xi(p)$, has been dropped in writing Eq. (5), since $v_1(\rho_\infty)$ must vanish; otherwise the function $\xi(p, \rho_\infty)$ has the same sign below and above the Fermi surface, and the Landau state becomes unstable before ρ reaches ρ_∞ .

Eq. (6) can be simplified using particle-number conservation, expressed approximately as

$$\int [p_F(p - p_F) + (p - p_F)^2] \frac{\partial n(\xi(p))}{\partial p} dp = 0. \quad (7)$$

Inserting this relation into Eq. (6), we have

$$\frac{M}{M^*(T, \rho)} = D(\rho) - v_2 \int \frac{(p - p_F)^2}{p_F^2} \frac{\partial n(\xi(p))}{\partial p} dp. \quad (8)$$

In terms of the new variables $\tau = 2TM/p_F^2$, $x = \xi(p)/T$ and $y = (p - p_F)(v_2/3MTp_F)^{1/3}$, Eq. (8) reduces to $M/M^*(T, \rho) = D(\rho) + \nu a \tau^{2/3}$, while Eq.(5) becomes

$$\frac{d\xi(p, T, \rho)}{dp} = \frac{p_F}{M} \left[D(\rho) + \nu \tau^{2/3} [a + y^2] \right], \quad (9)$$

which is recast to a relation between x and y ,

$$x = y \left[3\nu^{-1} D(\rho) \tau^{-2/3} + 3a + y^2 \right]. \quad (10)$$

where $\nu = (9v_2/4)^{1/3}$ and

$$a = \int_{-\infty}^{\infty} y^2(x) e^x (1 + e^x)^{-2} dx. \quad (11)$$

Having solved Eqs. (10) and (11), the polarization operator $\Pi_0 \equiv -N_0 P_0$ is straightforwardly evaluated to yield

$$\chi(T, \rho) = \mu_B^2 N_0 P_0(T, \rho) / [1 + G_0(\rho) D(\rho) P_0(T, \rho)], \quad (12)$$

where $G_0 = g_0 p_F M^*(T=0)/\pi^2$, and

$$P_0(T, \rho) = \int_{-\infty}^{\infty} \frac{e^x (1 + e^x)^{-2}}{[a(T, \rho) + y^2(x)] \nu \tau^{2/3} + D(\rho)} dx. \quad (13)$$

In what follows we address systems without ferromagnetic ordering where $1 + G_0 > 0$. In this case, $P_0(T, \rho)$ crucially depends on the ratio $T/|\rho - \rho_\infty|$. When T drops to 0 while $|\rho - \rho_\infty|$ is fixed, one obtains $P_0(T, \rho) = D^{-1}(\rho)$, and hence $\chi(T=0, \rho \neq \rho_\infty) = \mu_B^2 N_0 / [D(\rho)(1 + G_0)] \sim |\rho - \rho_\infty|^{-1}$. In the opposite case, $D(\rho_\infty) = 0$ and calculations yield $M/M^*(T, \rho_\infty) \simeq a(\rho_\infty) \nu \tau^{2/3}$, and $P_0(T, \rho_\infty) = b(\rho_\infty) \nu^{-1} \tau^{-2/3}$ with $a(\rho_\infty) = 0.5$ and $b(\rho_\infty) = 1.2$, so that

$$\chi(T, \rho_\infty) = \chi_0(T, \rho_\infty) = 1.2 \mu_B^2 N_0 \nu^{-1} \tau^{-2/3}. \quad (14)$$

This implies that the critical index α specifying the low- T dependence of the inverse spin susceptibility $\chi^{-1}(T, \rho_\infty)$ is $2/3$.

It can be verified that the corresponding 1D and 2D equations are identical in form to Eqs. (10) and (11), derived here for the 3D case.

The above treatment can be extended to other thermodynamic properties, e.g. the specific heat given by

$$C = -\frac{p_F^2}{\pi^2} \int \xi n(\xi) [1 - n(\xi)] \frac{dp}{d\xi} \frac{\partial}{\partial T} \left(\frac{\xi(T)}{T} \right) d\xi. \quad (15)$$

Manipulations similar to those applied to $\Pi_0(T, \rho)$ yield

$$\frac{C(T, \rho)}{T} = N_0 \int_{-\infty}^{\infty} \frac{x[x - 2ay(x)] e^x (1 + e^x)^{-2}}{[a + y^2(x)] \nu \tau^{2/3} + D(\rho)} dx. \quad (16)$$

Thus we see that at $T \rightarrow 0$ the ratio $C(T)/T$ possesses the same NFL behavior as the spin susceptibility.

In electron systems of solids, as a rule there exist several bands that cross the Fermi surface, the effective mass diverging only in one or two of them. Other bands still contribute as Landau theory dictates providing additional T -independent terms in $\chi(T)$ and $C(T)/T$ and modifying somewhat the prefactors in the singular parts. As a result, the behavior $T^{-2/3}$ implied by Eq.(14) holds in dealing with the T -dependent excesses $\Delta\chi(T, \rho_\infty)$ and $\Delta C(T, \rho_\infty)/T$. One may expect the same to be true for anisotropic systems, e.g. for 2D liquid ^3He , where the enhancement of M^* is associated with the crystal lattice of the substrate.¹⁹

To ascertain the relevance of the basic result (14) to real strongly correlated Fermi systems, we make use of data^{8,9,10} for the heavy-fermion metals $\text{YbRh}(\text{Si}_{0.95}\text{Ge}_{0.05})_2$ and CeRu_2Si_2 , where the T -independent FL terms are rather small. These data, as seen from the left panel of Fig. 1, are well reproduced by the proposed model.

In 2D liquid ^3He the FL term in $\chi(T)$ is significant. Accordingly, in the right panel of Fig. 1 we plot results for the excess $\Delta\chi(T)$ at the two densities $\rho = 0.036A^{-2}$ and $\rho = 0.052A^{-2}$. In doing so, we suggest that the flat portion in the spectrum $\xi(\mathbf{p})$ forms in certain regions adjacent to the Fermi line of ^3He , and these regions produce contributions $\Delta\chi(T) \sim T^{-2/3}$, while the remainder generates only the FL terms. We suggest that with increasing density the latter region shrinks and vanishes at the point where liquid ^3He solidifies. Our calculations are compared with experimental data¹ in the right panel of Fig. 1.

Let us now examine the role of damping effects. When evaluating thermodynamic properties, characteristic energies ε are of order of T . We estimate the damping $\gamma(\varepsilon \sim T)$ with the help of the standard FLT formula

$$\gamma(\varepsilon \sim T) \sim |\Gamma|^2 [M^*(T)]^3 T^2 \quad (17)$$

containing the interaction amplitude Γ and the effective mass M^* , which according to Eq. (9), depends on T as

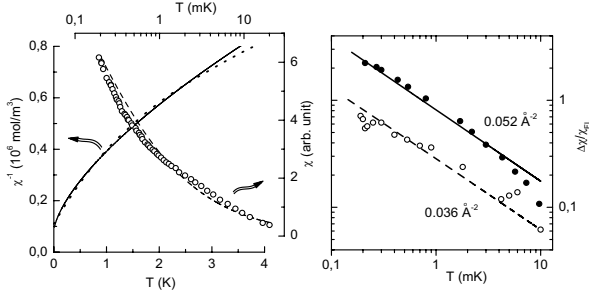


FIG. 1: Left panel, bottom-left axes: Inverse magnetic susceptibility of $\text{YbRh}(\text{Si}_{0.95}\text{Ge}_{0.05})_2$ as a function of temperature. Experimental data of Ref. 8 are shown as short dashes; the solid curve is the current prediction. Top-right axes: temperature dependence of magnetic susceptibility of CeRu_2Si_2 in a magnetic field of 0.02 mT. Experimental data of Ref. 10 are denoted by circles, and the theoretical prediction by the dashed curve. Right panel: Spin susceptibility excess, divided by the FL contribution to the spin susceptibility, evaluated for ^3He films at two densities (indicated near the curves). Experimental data from Ref. 2 appear as solid and open circles, while solid curves trace the predictions of the current theory at low T .

$T^{-2/3}$. It is important to recognize that the customary replacement¹⁷ of Γ by the bare interaction V , although legitimate in ordinary Fermi liquids, is erroneous in the limit of strong correlations. The source of the error is the huge enhancement of the density of states, which suppresses Γ and makes its magnitude quite insensitive to the bare interaction.¹⁸ To wit: summation of ladder diagrams in the particle-hole channel gives $\Gamma = V/[1 + VN(0)]$, where $N(0) \sim p_F M^*$ is the density of states. In the limit $N(0)V \gg 1$, one obtains $\Gamma \sim N^{-1}(0)$. Inserting this result into Eq. (17), we obtain

$$\gamma(\varepsilon \sim T)/T \sim TM^*(T)/p_F^2 \sim \tau^{1/3} \ll 1, \quad (18)$$

affirming the applicability of FLT theory to our problem.

Imposition of a static external magnetic field H brings into play a new dimensionless parameter $R = \mu_B H/T$ and opens another arena for testing the model. The function $n(\xi(p))$ entering Eq. (3) is then replaced by $[n(\xi_+(p)) + n(\xi_-(p))]/2$, where $n(\xi_{\pm}(p)) = [1 + \exp(\xi(p)/T \pm R/2)]^{-1}$. In turn, $\xi(p)$ is determined from Eq. (5), the effective mass being the same for both spin directions at sufficiently weak H . Proceeding as before, we find

$$M/M^*(T, H, \rho_\infty) = \nu \tau^{2/3} a(R), \quad (19)$$

where

$$a(R) = \frac{1}{2} \int y^2(x) \left[\frac{e^{x+R/2}}{(1+e^{x+R/2})^2} + \frac{e^{x-R/2}}{(1+e^{x-R/2})^2} \right] dx. \quad (20)$$

In the limit $T \rightarrow 0$ or equivalently $R \rightarrow \infty$, the solution of this equation takes the analytic form $M^*(T = 0, H, \rho_\infty) \sim H^{2/3}$, confirming a result of Ref. 16. Thus at

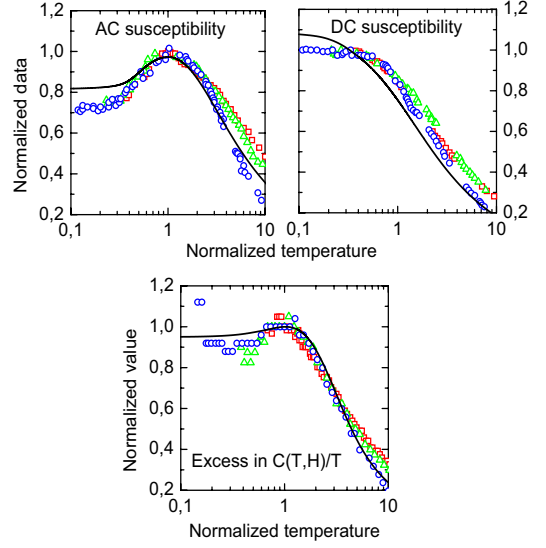


FIG. 2: Top panels: Normalized magnetic susceptibility $\chi(T, H)/\chi(T_P)$ (top-left panel) and normalized magnetization $\mathcal{M}(T, H)/\mathcal{M}(T_P)$ (top-right panel) for CeRu_2Si_2 in magnetic fields 0.20 mT (squares), 0.39 mT (triangles), and 0.94 mT (circles), plotted against normalized temperature T/T_P (Ref. 10), where T_P is the temperature at peak susceptibility. The solid curves trace the universal behavior predicted by the present theory. Bottom panel: The normalized ratio $C(T, H)T_M/C(T_M)T$ for $\text{YbRh}(\text{Si}_{0.95}\text{Ge}_{0.05})_2$ in magnetic fields 0.05 T (squares), 0.1 T (triangles), 0.2 T (circles) versus the normalized temperature T/T_M (Ref. 13), where T_M is the temperature at maximum ratio $C(T, H)/T$. The solid curve shows the prediction of our theory.

sufficiently low temperatures, imposition of static magnetic fields satisfying $\mu_B H > T$ renders the effective mass $M^*(T, H, \rho_\infty)$ finite, promoting the recovery of the Landau theory. Along the same lines, at the critical density ρ_∞ we may establish that the magnetic moment and AC spin susceptibility display a scaling behavior, e.g.

$$\chi_{AC}(T, H, \rho_\infty) = \mu_B^2 N_0 \nu^{-1} b(R) \tau^{-2/3}, \quad (21)$$

where

$$b(R) = \frac{1}{2} \int \left[\frac{e^{x+R/2}}{(1+e^{x+R/2})^2} + \frac{e^{x-R/2}}{(1+e^{x-R/2})^2} \right] \frac{dx}{a(R)+y^2(x)}. \quad (22)$$

Turning to the specific heat, and following the same path as taken above for $\chi(T, H)$ at the critical point, we are led to the expression

$$C(T, H, \rho_\infty)/T = N_0 \nu^{-1} c(R) \tau^{-2/3}, \quad (23)$$

where

$$c(R) = \frac{1}{2} \int \left[\frac{[(x+R/2)^2 - 2(x+R/2)a(R)y(x)]e^{x+R/2}}{(1+e^{x+R/2})^2} + \frac{[(x-R/2)^2 - (x-R/2)a(R)y(x)]e^{x-R/2}}{(1+e^{x-R/2})^2} \right] \frac{dx}{a(R)+y^2(x)}. \quad (24)$$

A scaling behavior of this kind has been discussed by Coleman and collaborators.^{6,12}

For finite H , the curve describing $\chi_{AC}(T, H)$ acquires a maximum at some temperature T_P , as does the curve for $C(T, H)/T$, at some temperature T_M . This behavior is associated with the suppression of the divergent NFL terms $\sim T^{-2/3}$ in $\chi(T, H)$ and $C(T, H)/T$ and recovery of the FL behavior at static magnetic fields in which the Zeeman energy splitting $\mu_B H$ exceeds T . Following Ref. 10 we present in Fig.2 the results of numerical calculations of these quantities as functions of the normalized temperatures T/T_P and T/T_M to demonstrate that our model reproduces the experimental scaling behavior of the spin susceptibility¹⁰ of the heavy fermion metal CeRu₂Si₂ and that of the specific heat¹³ of the heavy fermion compound YbRh(Si_{0.95}Ge_{0.05})₂, *without adjustable parameters*. It should be emphasized that the curves given in Fig.2 remain the same whether one is working with heavy fermion metals or 2D liquid ³He. This universality, predicted by our model, can be tested with the aid of a new apparatus²⁰ designed for measurements of thermodynamic properties of 2D liquid ³He in static magnetic fields.

It is worth noting that, as seen from Eq.(2), on the metallic side of the phase transition the NFL behavior (14) holds in a density domain $\Delta\rho \sim \rho_\infty \tau^{2/3}$ adjacent to the critical point. On the other hand, as we plan to demonstrate in our next article, on the insulating side of the phase transition, the range of the domain where the NFL term $\sim T^{-2/3}$ prevails is substantially larger, $\Delta\rho \sim \rho_\infty \tau^{1/3}$.

Let us compare our results with those available within the antiferromagnetic scenario.¹¹ First, the proposed flattening mechanism for NFL behavior adequately explains the low- T data on the spin susceptibility, producing $\chi^{-1}(T) \sim T^\alpha$ with $\alpha \simeq 2/3$ in the critical density region, while the SFM fails to provide $\alpha < 1$. Second, the flattening mechanism explains the scaling behavior $\chi^{-1}(T) \sim T^\alpha F(H/T)$ of the spin susceptibility in static magnetic fields, whereas such a scaling property does not arise in the SFM. Third, within the model developed here, FL behavior can be recovered at low T close the critical point by imposing a tiny magnetic field satisfy-

ing $\mu_B H > T$. In the SFM there is no such provision for reinstating Fermi-liquid theory.

Finally, we discuss the relevance of ferromagnetic fluctuations to the NFL behavior, claimed in Refs. 9,10. Experimental data for most heavy-fermion systems show no evidence of ferromagnetism. The same is true for 2D liquid ³He.^{1,3} This implies that close to the critical point, the respective Pomeranchuk stability condition¹⁵ $1 + G_0(\rho) > 0$ is not violated, in spite of the divergence of the effective mass at $\rho = \rho_\infty$. The value of G_0 can be estimated from the Landau sum rule¹⁵ $\sum_L \{F_L/[1+F_L/(2L+1)]+G_L/[1+G_L/(2L+1)]\} = 0$ by assuming all the harmonics F_L to be finite, apart from $F_1=F_1^0 M^*/M \simeq 3M^*/M$. The Landau sum rule is then satisfied provided $G_0 \simeq -0.75$. This value of G_0 gives rise to a marked enhancement of the Sommerfeld ratio in the case $\mu_B H > T$, to a around 12 that changes little if the zeroth harmonic F_0 is taken into account. Even so, such an enhancement does not in itself ensure the relevance of ferromagnetic fluctuations to the NFL behavior. Indeed, dense 3D liquid ³He, in which $G_0 \simeq -0.8$, shows no deviations from FLT predictions as $T \rightarrow 0$.

In summary, we have studied the impact of flattening of the single-particle spectrum on the spin susceptibility $\chi(T)$ and the specific heat $C(T)$ of strongly correlated Fermi systems. When the density approaches the critical value at which effective mass becomes infinite, Fermi-liquid theory progressively fails as the deviant components in $\chi(T)$ and $C(T)$ grow to dominance. We have explicated the implied critical behavior of these components and derived a universal relation between them. Finally, our analysis has revealed the scaling behavior of $\chi(T, H)$ and $C(T, H)/T$ in the presence of an external magnetic field H . Numerical results based on this theoretical picture are in agreement with experimental data on 2D liquid ³He and several heavy-fermion metals.

We thank L. P. Gor'kov, G. Kotliar, E. Krotscheck, V. R. Shaginyan, and V. M. Yakovenko for valuable discussions. This research was supported by NSF Grant PHY-0140316, by the McDonnell Center for the Space Sciences, and by Grant NS-1885.2003.2 from the Russian Ministry of Education and Science.

¹ C. Bäuerle *et al.*, J. Low Temp. Phys. **110**, 333 (1998).

² C. Bäuerle *et al.*, J. Low Temp. Phys. **110**, 345 (1998).

³ A. Casey *et al.*, J. Low Temp. Phys. **113**, 293 (1998).

⁴ S. V. Kravchenko and M. P. Sarachik, Rep. Prog. Phys. **67**, 1 (2004).

⁵ O. Prus *et al.*, Phys. Rev. **B 67**, 205407 (2003).

⁶ A. Schröder *et al.*, Nature **407**, 351 (2000).

⁷ G. R. Stewart, Rev. Mod. Phys. **73**, 787 (2001).

⁸ R. KÜchler *et al.*, Phys. Rev. Lett. **91**, 066405, (2002).

⁹ P. Gegenwart *et al.*, Acta Phys. Pol. **B34**, 323 (2003).

¹⁰ D. Takahashi *et al.*, Phys. Rev. **B67**, 180407, (2003).

¹¹ A. J. Millis, Phys. Rev. **B48**, 7153 (1993).

¹² P. Coleman and C. Pepin, Physica **B 312-313**, 383 (2002).

¹³ J. Custers *et al.*, Nature **424**, 524 (2003).

¹⁴ R. KÜchler *et al.*, cond-math/04077981.

¹⁵ L. D. Landau and E. M. Lifshitz, *Statistical physics*, Vol. 2 (Pergamon Press, Oxford, 1980).

¹⁶ V. R. Shaginyan, JETP Lett. **77**, 99 (2003); **79**, 344 (2004).

¹⁷ P. Nozières, J. Phys. I France **2**, 443 (1992).

¹⁸ J. Dukelsky *et al.*, Z. Phys. **B102**, 245 (1997).

¹⁹ M. Morishita, H. Nagatani, and H. Fukuyama, J. Low Temp. Phys. **113**, 299 (1998).

²⁰ C. Matsumoto *et al.*, Physica **B 329-333**, 146 (2003).